PAPER

The effects of long and bulky aromatic pendent groups with flexible linkages on the thermal, mechanical and electrical properties of the polyimides and their nanocomposites with functionalized silica†

Simi Annie Tharakan [ID] * and Sarojadevi Muthusamy

A novel diamine bis(4-aminophenyl)bis{3,4[(4-(8-quinolyloxymethyl carbonyl)]}methane, containing two long/bulky aromatic pendent chains was synthesized by incorporating aromatic and hetero aromatic groups with flexible linkages. Flexible, stretchable, thermally stable and processable polyimides were prepared by reacting this newly synthesized diamine with commercial tetracarboxylic acid dianhydrides like 3,3′,4,4′-benzophenone tetra carboxylic acid dianhydride (BTDA) and 4,4′-(4,4′-isopropylidenediphenoxy)diphthalic Anhydride (BPADA). Nanocomposites of polyimides were prepared using aromatic amine functionalized silica as a filler by solution casting method. The current work investigates the effects of incorporating long/bulky aromatic side chains and flexible linkages on the thermal, mechanical, electrical and optical properties of the polyimides and nanocomposites. The polyimides showed good thermal stability ($T_{10\%}$ = 364 & 388), high flame resistance, low glass transition temperatures (T_g = 130 °C & 156 °C), very low dielectric constants (2.5 & 2.8 at 1 MHz) and good optical transparency. The neat polyimides displayed good elongation at break (133–155%) but possessed low tensile strength. The chemically imidized polyimides showed good solubility in low and high boiling solvents. Nanocomposites of polyimides based on aromatic amine functionalized silica exhibited enhanced properties with $T_{10\%}$ values varying between 409–482 °C, T_g between 165–280 °C and higher dielectric constants (3–5.7 at 1 MHz).

Introduction

Aromatic polyimides are well recognized as high performance materials due to their excellent thermal mechanical and dielectric properties. Conventional polyimides are used in various fields like automobile, aerospace, electrical, electronics and packaging industries in different forms like coatings, composites, insulating films, adhesives, membranes, and sealants.[1–3] But their applications are limited as they meet difficulties in processing due to their poor solubility in organic solvents and high melt/glass transition temperatures in the fully imidized form.[4] Another major problem is the deep color and poor optical transmittance of the polyimides, making them non-suitable candidates for optoelectronics.[5] All these are due to the rigidity and high crystallinity of the polymer chain backbone which is the result of the inter chain interaction and cohesive forces causing the formation of charge transfer

complex formation, in their highly conjugated structures. There are many approaches to make structural modifications and to tailor desired properties. Those are introducing flexibilizing linkages in the chain backbone and attaching long and bulky groups, making coplanar and unsymmetrical structures or copolymerization.[4]

The factors or different approaches leading to better solubility and lower transition temperatures often conflict with some requirements for high performance applications of the polymers, such as high thermo-mechanical properties and chemical resistances. Ether linkages will increase the localized segmental rotation and improve the solubility, without sacrificing much of the good thermal stabilities. The methylene or isopropylidene linkages will decrease the glass transition temperature and thermo-oxidative stability will be compromised. Amutha *et al.* reported that the bulky poly cyclic aryl group like anthracene in the side chain can impart elevated T_g and good thermal and mechanical properties with better solubility in the organic solvents.[6,7] Wang *et al.*[8] reported that the inclusion of long and bulky multiple alkyl side chains impart excellent solubility, toughness, flexibility and good elongation even above 200% *i.e.* stretchability or elastomeric properties can

Department of Chemistry, CEG, Anna University, Chennai, India 600025. E-mail: msrde2000@yahoo.com; tharakansat@gmail.com

be imparted in the polyimides but with inferior thermal and mechanical properties. But, it has been established that the bulky aryl groups in the main and side chains impart good thermal stability and mechanical strength.[9–11] Most of the measures mentioned above modified the conventional polyimides to an easily processable material with totally different and large varieties of applications like OLED,[5] thin film transistors, thin film solar cell or photo voltaics,[12] FPCB with new colourless polyimides, electro chromic materials,[13,14] LB films, polymeric memory,[15] photoresists, sensors, capacitors and solid poly electrolytes for fuel cells or batteries.[16–20] They are used as membranes for gas separations[21] in power plants and oil refineries.

At the same time elastomers are excellent and relatively cheap materials for various applications in many sectors including automotive, industrial, packaging and healthcare.[22] Always there are requirements for elastomers with high T_g and thermal stability. There is a need of the new varieties of insulator for the aircraft and missile combustor case related to the aerodynamic heating. Silicone, with a T_g of -127 °C the material used for this purpose, has reached performance limitations. KALREZ, from DuPont is the most thermally stable commercially available fluoroelastomer, with a continuous service temperature above 260 °C.[23] Recently many kinds of elastomers were reported. Ramdas *et al.* reported shape memory polytriazole elastomers from aromatic monomers which exhibited T_g of 35 °C, an elongation of about 80%, a shore A hardness of 55 and a T_5 above 250 °C.[24] Chen *et al.* reported a highly stretchable, self-healing, and 3D printing hydrogels with tensile strength, elongation at break, and Young's modulus of 61.0–103.4 kPa, 1150–1560%, and 42.7–125.7 kPa, respectively.[25] Parmeggiani *et al.* reported a novel kind of PDMS/polyimide composite as elastomeric substrate for multifunctional laser-induced graphene electrodes for flexible electronic applications.[26] Until now, not much research works were carried out to prepare thermally stable, stretchable polyimides from aromatic monomers. Thereby researches are required to develop a new material which incorporates the noble properties of polyimide and elastomers. Otherwise, by synthesizing new kinds of elastomers from the polyimides which are tailor made or with desired properties *i.e.* materials with good solubility, optimum T_g, good thermal stability, tensile strength and elongation, depending on their various service requirements. In one of our recently published work, the polyimide having single pendent groups exhibits high elongation at break of 260%.[27] The effect of side groups in the polyimide chain backbone on thermal, mechanical and electrical properties were investigated in detail by Meise *et al.*[28] and Deng *et al.*[29]

Organic/inorganic hybrid composites which combine advantages of organic polymers with the benefits of inorganic materials became an area of extensive research in the recent years.[30,31] Incorporation of SiO_2 nanoparticles, in the form of intercalation or exfoliation was found to improve thermal stabilities as well as mechanical strength (showed improved hardness and modulus), gas barrier properties, flame resistance and electrical properties.[32] These materials act as a heat sink and protect polymer matrix from undergoing decomposition in

the normal pattern. Enhancement in the properties is based on the strong interaction of nanoparticles and polyimide matrix along with the well-defined and uniform dispersion of particles in the matrix.[33,34] Silica nano particle has high surface energy along with the hydrophilic hydroxyl groups on the surface which leading to self-assembly of them resulting in aggregation and low compatibility with the hydrophobic polymer matrix. In order to improve the compatibility of the nano materials with polymer, surface modification is widely used using a silane coupling agent which has amino group such as 3-amino propyl triethoxy silane (APTES), phenyl trimethoxy silane(PTMS), 3-trimethoxy-silylpropyl) diethylenetriamine (DETAS).[35–37] But aliphatic groups in these coupling agents reduce the thermal stability. Taeho Kang *et al.* in 2016 (ref. 38) reported the surface modification of silica with PTMS and it shows increased hydrodynamic volume. Taeho Kang *et al.* in 2017 (ref. 39) and Ghorpade *et al.* in 2015 (ref. 40) reported the preparation of nanocomposites based on phenyl amino functionalized silica in which nanoparticles were dispersed without agglomeration. Modification of the silica nanoparticles with *p*-aminophenyl trimethoxysilane (APhTMS) was observed to maintain and enhance thermal, and mechanical properties of the polyamide-imide matrix.[39] The weight percentage of nanosilica and its mode of dispersion in the polyimide matrix has tremendous effect on thermal and electrical properties of polyimide nanocomposites.[41]

The objective of this study is to investigate the effects of two long/bulky side chains containing aromatic/hetero aromatic groups and flexible linkages, on the thermal, mechanical and electrical properties, along with the processability of the polyimides. It has been observed that the incorporation of long and/ or bulky aromatic sidechains and flexible linkages may generate highly amorphous polyimide matrix with improved free volume resulting in good flexibility/stretchability while retaining good thermal and mechanical properties. To achieve the same, a diamine having two long/bulky side chains with aromatic and heteroaromatic groups along with ether, keto and methylene linkages, was prepared. Polyimides were prepared with selected aromatic dianhydrides like 3,3′,4,4′-benzophenone tetra carboxylic acid dianhydride (BTDA) and 4,4′-(4,4′-iso-propylidenediphenoxy) diphthalic anhydride (BPADA) to incorporate isopropylidene and keto groups in the polymer main chain. The nanocomposites were prepared by direct blending of the sonicated suspension of aromatic amine functionalized silica nano powder in NMP to the poly (amic acid) solution followed by the thermal imidization method. The obtained polyimides were subjected for detailed investigation on thermal/mechanical/electrical/optical properties and solubility. The detailed study of the nanocomposites on their morphology, and thermo-electrical properties is discussed.

Experimental

Materials

3,4-Dihydroxy benzaldehyde, *p*-hydoxy benzaldehyde and diamino diphenyl methane were purchased from Spectrochem Pvt. Ltd, India. Aniline and acetic anhydride (Fischer, India) were

used as received. 3,3′,4,4′-Benzophenone tetra carboxylic acid dianhydride (BTDA, Acros, India) and bisphenol-A dianhydride (BPADA, Sigma Aldrich, USA) were recrystallized from acetic anhydride. All the reaction solvents such as dimethyl formamide (DMF), N,N-dimethyl acetamide (DMAc), N-methyl pyrollidone (NMP), dimethyl sulphoxide (DMSO), toluene, acetone, chloroform, and tetrahydrofuran (THF), were purified by appropriate method. Ethanol was purified by stirring with calcium carbonate for 12 hours followed by distillation under atmospheric pressure. 8-Hydroxy quinoline, acetanilide, silicon dioxide nano powder (15 nm) were purchased from Sisco Research Laboratories Pvt. Ltd (SRL). Concentrated hydrochloric acid, methanol and isopropyl alcohol were received from Spectrum private limited (Cochin, Kerala). 2,4′-Dibromo acetophenone (Alfa Aser India Private Limited), potassium iodide (MERCK, India), sodium nitrite (Spectrochem, India), potassium carbonate, pyridine (MERCK, India) was used as received.

Characterization methods

FT-IR spectra were recorded on a Perkin Elmer RX1 spectrometer with KBr pellet. ^{1}H-NMR and ^{13}C-NMR spectra were recorded using a JEOL Ex-400 spectrometer with CDCl$_3$ or DMSO as solvent and tetra methyl silane (TMS) as reference. Thermograms were obtained using TA instruments Q50V20 series thermogravimetric analyzer at a heating rate of 10 °C min^{-1} in with a nitrogen flow of 60 ml min^{-1}. Differential scanning calorimetry was used to determine the T_g of the polymers using a NETZSCH DSC 204 instrument at a heating rate of 10 °C min^{-1} from 40 to 400 °C with a nitrogen flow of 60 ml min^{-1}. Solubility of the polymers was tested in various solvents by mixing 2–3 mg of the polymer with 8 mL of the solvent and kept aside for 24 hours with occasional shaking. If the mixture was insoluble under cold conditions, then it was heated and cooled. Inherent viscosity measurements were conducted at 25 °C in DMAc solvent using Cannon Ubbelohde viscometer. The weight-average molecular weights (M_w) and number average molecular weights (M_n) were obtained via gel permeation chromatography (GPC) on the basis of polystyrene calibration on a PL-GPC 220 instrument with DMF as an eluent at a flow rate of 1.0 mL min^{-1}. Wide angle X-ray diffraction measurements were performed at room temperature (about 25 °C) on an X-pert PAN analytical X-ray diffractometer using Ni-filtered Cu Kα radiation. The scanning rate was 20° min^{-1} over a range of $2\theta = 5°–70°$. Mechanical properties of the films were measured with an Instron model 1130 tensile tester using a 5 kg load cell at a cross head speed of 5 mm min^{-1} on strips of approximately 1 mm thick and 5 mm width with a 15 mm gauge length by the standard ASTM D638. Dielectric properties were measured with the help of an impedance analyzer (Solatron 1260 Impedance Gain phase Analyzer, UK) at room temperature. The polymer samples were cut in to circular shape (of size 1 mm thickness and 10 mm diameter) using a platinum electrode sandwich model in the frequency range of 100 Hz to 1 MHz. The morphology of the material was examined by scanning electron microscope (SEM) (JEOL, JSM-5600) at an accelerating voltage of 20 keV. Photomicrographs were taken on the

surface, which was made by breaking the specimen by impact testing machine and then coating with gold powder. Transmission electron microscopic (TEM) images were recorded using JEOL TEM-3010 electron microscope operated at an accelerating voltage of 300 keV. The samples for TEM image were prepared by dispersion of the material in ethanol under sonication and deposited on a copper grid. The absorption spectra were recorded between 200 and 800 nm on Shimadzu (1650) UV-vis spectrophotometer using dimethyl acetamide as solvent.

Synthesis of bis(4-aminophenyl)bis{3,4[(4-(8-quinolyloxymethyl carbonyl)phenoxy]}methane [BAPQMCPM]

Synthesis of bis(4-acetamido phenyl)3,4-dihydroxy phenyl methane [BAPDPM]. In a 500 ml round bottomed flask equipped with a magnetic stirrer bar, nitrogen inlet and reflux condenser, acetanilide (1.957 g, 0.0145 mol) was taken and dissolved in 10 ml of DMF. To that concentrated HCl (2 ml, excess than 0.0145 mol) was added drop wise, while the round bottomed flask was maintained at 0 °C. After the completion of HCl addition, 3,4 dihydroxy benzaldehyde (1 g, 0.00725 mol) dissolved in 10 ml of DMF was added to the reaction mixture drop by drop for a period of half an hour. The reaction mixture was allowed to come to room temperature, heated to 120 °C and maintained at this temperature with stirring for 12 hours (Scheme 1). The reaction mixture was finally cooled to room temperature, 5% solution of sodium bicarbonate was added dropwise until precipitation started and kept in the refrigerator overnight when the precipitation was completed. The brown coloured precipitate thus formed was collected by filtration, washed with methanol and 5% solution of sodium bisulphite, and dried in a vacuum oven at 60 °C for 12 hours. The crude product was recrystallized from DMF/water system. Yield 70%, M.P.128 °C. FT-IR (KBr, cm^{-1}): 3364 (broad band, asymmetric and symmetric stretching vibrations of hydroxyl group, 3286 (asymmetric and symmetric stretching vibrations of amide –NH group.), 3024 (aromatic C–H stretching vibrations) 2916 (aliphatic C–H stretching) 1628 (N–H in-plane bending vibrations), 2793 (vibrations of bridging –CH group), 1669 (symmetrical stretching vibrations of amide C=O). ^{1}H-NMR (DMSO-d$_6$, ppm): 2 (6H, s, H$_a$), 8.8 (2H, s, H$_b$), 7 (4H, d, H$_c$), 7.2–7.6 (4H, d, H$_d$), 5.2 (1H, s, H$_e$, 6.7 (1H, dd, H$_f$), 6.5 (1H, d, H$_g$), 6.3 (1H, d, H$_h$), 10 (2H, s, H$_i$ & H$_j$).

Synthesis of (4-bromophenyl)-2-(quinolin-8-yloxy) methyl ketone [BPQMK]. Mono bromo pendent group was prepared by the following method (Scheme 1). 8-Hydroxy quinoline (2 g, 0.0138 mol) was taken in a 500 ml RB flask equipped with a magnetic stirrer and reflux condenser in an inert atmosphere and dissolved in 15 ml of DMF. To this 3.8121 g (0.0138 moles) of K$_2$CO$_3$ and a pinch of potassium iodide as catalyst were added. 2,4-Dibromo acetophenone (7.6 g, 0.0138) dissolved in 40 ml of DMF was then added to the above reaction mixture drop by drop over a period of 30 minutes and then heated in an oil bath for 24 hours maintaining a temperature of about 70 °C. The reaction mixture was cooled and precipitated by pouring in to a large excess of ice-cold distilled water and neutralized.

Paper
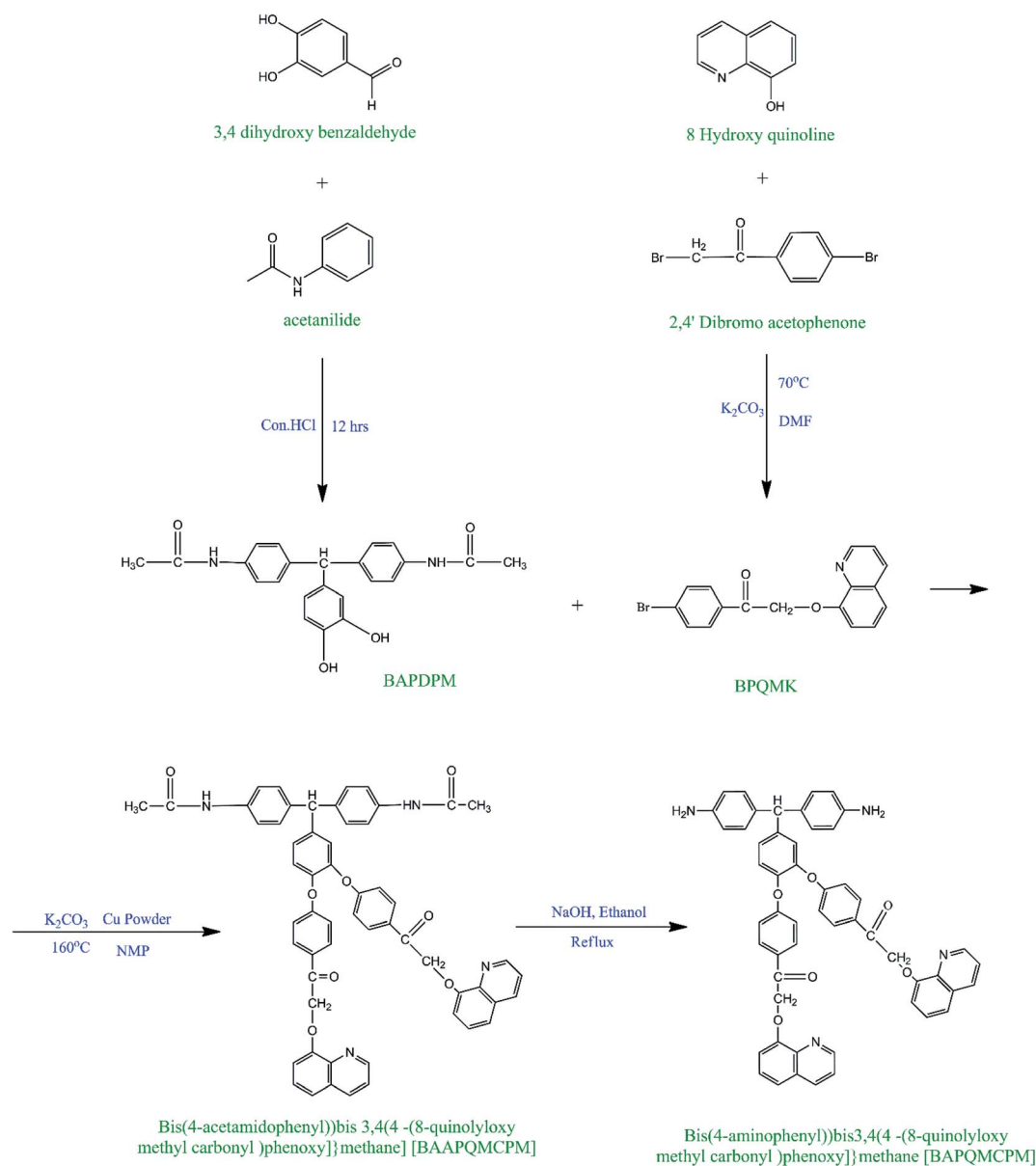
Scheme 1 Synthesis of bis(4-aminophenyl)bis{3,4[4-(8-quinolyloxy methyl carbonyl)phenoxy]}methane [BAPQMCPM].

Then, the precipitate was filtered and washed with water and dried under vacuum at 60 °C. The crude product was recrystallized from acetone/methanol mixture. Yield 85%. M.P 104 °C. FT-IR (KBr, cm^{-1}): 3061 (weak band, stretching vibrations of aromatic C–H group. 2923 (aliphatic C–H stretching) 1588 (aromatic in-plane bending vibrations), 1666 (symmetrical stretching vibrations of C=O group) 1246, 1100, 1069 (stretching vibration of C–O–C groups).

Synthesis of bis(4-acetamidophenyl)bis{3,4[4-(8-quinolyloxy methyl carbonyl)phenoxy]} methane [BAAPQMCPM]. Inert atmosphere was created by purging N$_2$ in the RB flask equipped with a magnetic stirrer, condenser and guard tube. BAPDPM (2 g, 0.0051 mole) was taken and dissolved in 35 ml NMP. Then, K$_2$CO$_3$ (1.4138 g, 0.0051 mole) and 2 wt% (0.05 g) of copper powder were added. Finally, synthesized BPQMK (3.5 g, 0.0103

moles) dissolved in 30 ml of NMP was added to the reaction mixture drop wise over a period of 30 minutes. The reaction mixture was heated in an oil bath for 24 hours maintaining a temperature of 160 °C, cooled, filtered to remove the copper powder and precipitated by pouring in to a large excess of ice-cold distilled water and neutralized carefully by adding dil. HCl in drops. The precipitate formed was then filtered, washed with methanol and 5% sodium bisulphite solution to remove the impurities and finally with water. The precipitate was then dried under vacuum oven at 60 °C. The crude product was recrystallized from DMF/water mixture. Melting point: 230 °C, Yield is 60%. FT-IR (KBr, cm^{-1}): 3302 (asymmetric and symmetric stretching vibrations of –NH group of secondary-amide group), 3055 (aromatic C–H stretching vibrations), 2924 (aliphatic C–H stretching of –CH$_2$ group), 1628 (N–H in-plane

bending vibrations), 2770, 2862 (presence of bridging –CH group) 1659 (symmetrical stretching vibrations of amide C=O group) 1720 (the stretching vibration of ketonic C=O group), 1072, 1250 (stretching vibration of aryl C–O–C group), 1597 (aromatic ring stretching). ^{1}H-NMR (DMSO-d_6, ppm): 2 (6H, s, H_a), 9.92 (2H, s, H_b), 7.96 (4H, d, H_c), 7.52 (4H, d, H_d), 5.7 (1H, s, H_e), 7.04 (1H, dd, H_f), 7.29 (1H, d, H_g), 7.37 (1H, d, H_h), 7.69 (2H, d, H_i), 8.61 (2H, d, H_j), 6.7 (2H, s, H_k), 7.44 (2H, dd, H_l), 8.23 (2H, t, H_m), 7.85 (2H, dd, H_n), 8.76 (2H, dd, H_o), 7.71 (2H, t, H_p), 8.93 (2H, dd, H_q).

Synthesis of bis(4-aminophenyl)bis{3,4[4-(8-quinolyloxy methyl carbonyl)phenoxy]}methane [BAPQMCPM]. The diamide compound BAAPQMCPM was hydrolyzed and converted in to the desired diamine BAPQMCPM. For hydrolysis, BAAPQMCPM (5 g, 0.00548 mole) of was taken in a 500 ml RB flask equipped with magnetic stirrer and reflux condenser. Ethanol (30 ml of 95%) and NaOH (2.2 g, 0.0548 mole) were added to the reaction mixture and refluxed for 24 hours (Scheme 1). Then, the reaction mixture was cooled and neutralized carefully with dil. HCl to precipitate the product. The precipitated product was filtered, washed with acetone and methanol and finally with water to remove the impurities and dried in a vacuum oven at 60 °C. Crude product was recrystallized using DMF/water (4 : 1) mixture. Yield 76%. M.P. 180 °C. FT-IR (KBr, cm^{-1}): 3443, 3426 (asymmetric and symmetric stretching vibrations of amino group, (aromatic C–H stretching vibrations) 2924, 2854 (aliphatic C–H stretching of –CH$_2$ group. 1628 (N–H in-plane bending vibrations), 1660 (symmetrical stretching vibrations of C=O group) 1111, 1070, 1257 (stretching vibration of Ar–O–Ar and Ar–O–R groups), 1597 (aromatic ring stretching). ^{1}H-NMR (DMSO-d_6, ppm): 2.9 (4H, s, H_a), 7.1 (2H, d, H_b), 7.2 (2H, d, H_c), 5.34 (H, s, H_d), 7.36 (1H, m, H_e), 7.45 (1H, m, H_f), 7.5 (1H, d, H_g), 7.6–7.7 (4H, d, H_h), 7.87 (4H, d, H_i), 6.8 (4H, s, H_j), 7.95 (2H, dd, H_k), 8.45 (2H, t, H_l), 8.1 (2H, dd, H_m), 7.99 (2H, dd, H_n), 8.6 (2H, t H_o), 8.99 (2H, dd, H_p). ^{13}C-NMR (DMSO-d_6, ppm): C_1 – 148.0, C_2 – 128.94, C_3 – 130.1, C_4 – 140.96, C_5 – 72.62, C_6 – 147.98, C_7 – 136.47, C_8 – 137.1, C_9 – 151.3 166, C_{10} – 149.4 164, C_{11} – 132.6, C_{12} – 162.6, C_{13} – 132.1, C_{14} – 132, C_{15} – 136.7, C_{16} – 194.3, C_{17} – 89.7, C_{18} – 164.5, C_{19} – 133.17, C_{20} – 129.8, C_{21} – 132.6, C_{22} – 151.3, C_{23} – 128.89, C_{24} – 129.12, C_{25} – 159.9, C_{26} – 161.2.

Preparation of aromatic amino functionalized silica nanoparticles

Aromatic amino functionalized nano silica particles were synthesized following a reported procedure[38] (Scheme S1†).

Synthesis of BAPQMCPM based polyimides

Synthesis of BAPQMCPM/BTDA-PI. BAPQMCPM (2.75 g, 0.0033 mol) was dissolved in 7 ml of NMP. After the diamine was completely dissolved, BTDA (1.1 g, 0.0033 mol) of was added to it. The reaction mixture was stirred at room temperature in nitrogen atmosphere for 16–18 hours. One portion of the obtained poly (amic acid) solution was spread on Petridish and placed in an oven at 80 °C overnight to remove the solvent. The semidried poly(amic acid) film was subjected to thermal imidization by heating from 100 °C to 300 °C in a sequential method 1 hour each at 120 °C, 150 °C, 200 °C, 250 °C, 30 minutes each at 275 °C and 300 °C to get a continuous, creasable polyimide film. Acetic anhydride (5 ml) and pyridine (2.5 ml) were added (2 : 1 v/v) to the remaining poly(amic acid) solution in chemical imidization method, and the mixture was stirred well for 8 hours at
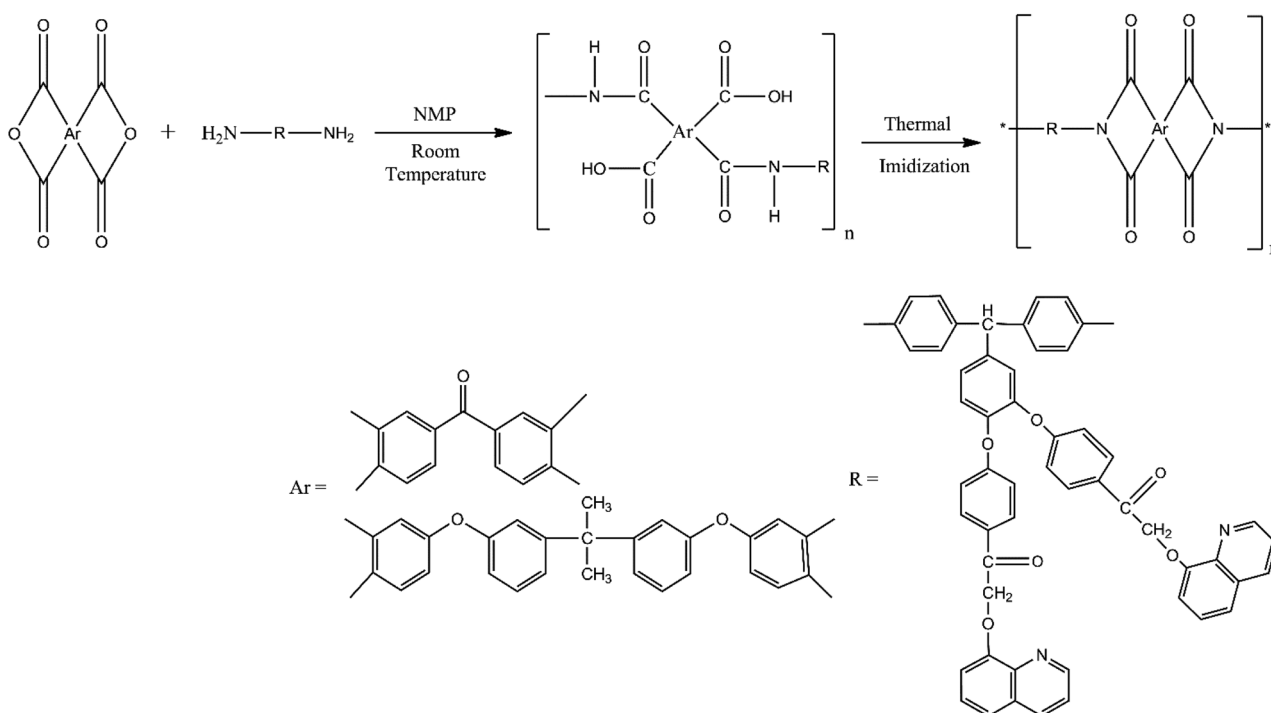
Scheme 2 Synthesis of BAPQMCPM based polyimides.
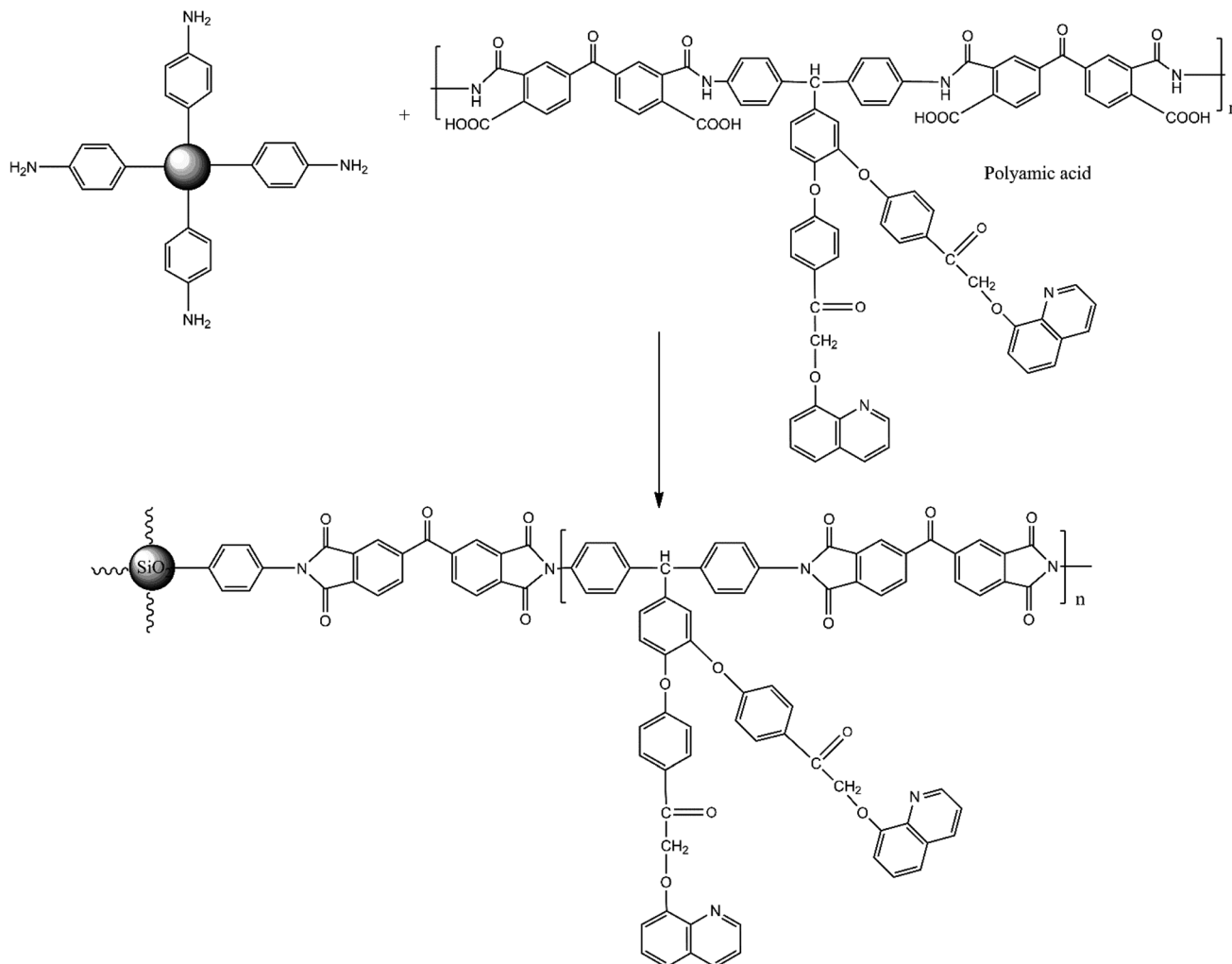
Scheme 3 Preparation of BAPQMCPM–BTDA/functionalized silica nanocomposites.

a temperature of 100 °C to achieve a complete imidization. The viscous solution was poured in to methanol to get brown coloured polyimide which was filtered, washed with hot methanol and dried in vacuum oven at 60 °C for 12 h (Scheme 2). FT-IR (KBr, cm^{-1}): 1774, 1712 (asymmetric and symmetric stretching of imide carbonyl group), 1362 (C–N–C stretching vibrations) 1155, 708 (C–N–C bending vibrations), 1160 (C–O–C stretching vibrations), 3050 (aromatic C–H stretching vibrations), 2960, 2916 (C–H stretching of methylene and methine group), 1655 (carbonyl group of BTDA and pendent group in the diamine) 1212, 1081 (Ar–O–Ar vibrations). ^{1}H-NMR (DMSO-d$_6$, ppm): 7–8.8 (m, 42H, aromatic protons), 6.2 (s, 2H, CH$_2$ protons) 5.5 (s, 1H, methine CH).

Synthesis of BAPQMCPM/BPADA-PI. The BAPQMCPM/BPADA-PI was prepared by adopting the same procedure used for the preparation of BAPQMCPM/BTDA-PI given above FT-IR (KBr, cm^{-1}): 1773, 1715.35 (asymmetric and symmetric stretching of imide carbonyl group), 1364 (C–N–C stretching vibrations), 1161, 708 (C–N–C bending vibrations), 1266 (C–O–C stretching vibrations), 3051 (aromatic C–H stretching vibrations), 2962, 2921 (C–H stretching of isopropylidene, methine,
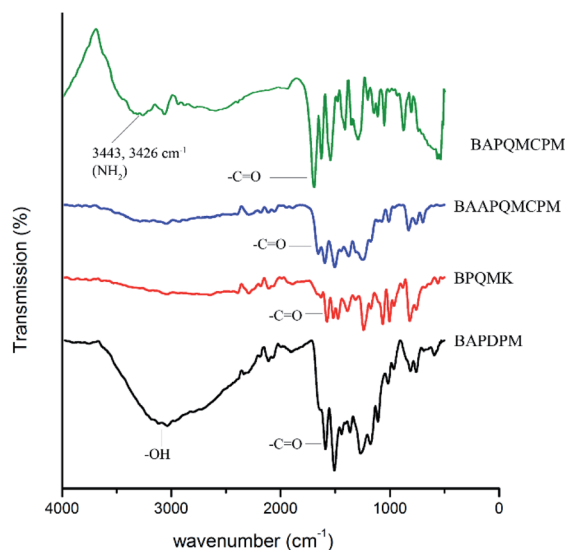

Fig. 1 FT-IR spectra of BAPDPM, BPQMK, BAAPQMCPM, BAPQMCPM.

and methylene groups). ^{1}H-NMR (DMSO-d$_6$, ppm): 7–8.5 (m, 54H, aromatic protons), 6.9 (s, 2H, OCH$_2$ protons), 5.3 (s, 1H, methine CH), 2.8 (s, 6H, isopropylidene protons).

Synthesis of BAPQMCPM/BTDA polyimide/aromatic amine functionalized silica nanocomposites. 2.75 g (0.0033 mol) of BAPQMCPM was dissolved in 7 ml of NMP. After the diamine was completely dissolved, (1.1 g, 0.0033 mol) of BTDA was added to it. The reaction mixture was stirred at room temperature in nitrogen atmosphere for 16–18 hours. From the total weight of diamine and dianhydride 2% was calculated and same 2% weight of SiO$_2$ in NMP was sonicated in an ultrasonic bath. It was then mixed with poly(amic acid) solution and sonicated again for 2 hours. The solution was poured in a Petridish, solvent was evaporated at 80 °C overnight and kept at 120 °C, 150 °C, 200 °C, 250 °C for one hour at each temperature and at 275 °C and 300 °C for half an hour each to complete the imidization. Similarly, 5% and 10% PI/SiO$_2$ nanocomposites were also prepared using the above procedure. Continuous and creasable nanocomposite films were formed[36] (Scheme 3).

BAPQMCPM/BTDA-PI/2%SiO$_2$ nanocomposites. FT-IR (KBr, cm^{-1}): 1777, 1716 (asymmetric and symmetric stretching of imide carbonyl groups), 1362 (C–N–C stretching vibrations) 1160, 800 (C–N–C bending vibrations) 1151, 1206 (C–O–C stretching vibrations), 3057 (aromatic C–H stretching vibrations), 2911 (C–H stretching of isopropyl and methylene group), 1658 (carbonyl group in the pendent group of diamine), 1048 (broad and strong band of Si–O–Si linkage), 710 (presence of long chain). The FT-IR spectrum of BAPQMCPM/BTDA-PI/5% SiO$_2$ and BAPQMCPM/BTDA-PI/10%SiO$_2$ nanocomposite also was found to have similar characteristic absorption bands like BAPQMCPM/BTDA-PI/2%SiO$_2$ nanocomposites.

Synthesis of BAPQMCPM/BPADA poly imide/aromatic amino functionalized silica nanocomposites. The BAPQMCPM/BPADA poly imide/aromatic amino functionalized silica (2%, 5%, and 10%) nanocomposites were prepared by adopting the same

procedure used for preparing BAPQMCPM/BTDA nano-composites. FT-IR (KB(r, cm^{-1}): 1772, 1714 (asymmetric and symmetric stretching of imide carbonyl groups), 1364 (C–N–C stretching vibrations) 1160, 749 (C–N–C bending vibrations), 1160, 1205 (C–O–C stretching vibrations), 3051 (aromatic C–H stretching vibrations), 2960, 2916 (C–H stretching of isopropyl and methylene group), 1660 (carbonyl group in the pendent group of diamine), 1070 (Si–O–Si linkage), 711 presence of long chain). The FT-IR spectrum BAPQMCPM/BPADA-PI/5%SiO$_2$ and BAPQMCPM/BPADA-PI/10%SiO$_2$ nanocomposite also was found to have similar characteristic absorption bands like BAPQMCPM/BPADA-PI/2%SiO$_2$ nanocomposites.

Results and discussion

Monomer synthesis

The diamine bis(4-aminophenyl)bis{3,4[4-(8-quinolyloxy methyl carbonyl)phenoxy]}methane [BAPQMCPM]was synthesized using a four-step reaction. In the first step, BAPDPM was prepared by the reaction of 3,4 dihydroxy benzaldehyde with acetanilide in the presence of concentrated hydrochloric acid in 1 : 2 molar ratios. Here, acetanilide is used to protect the amino group in the amide group form. The FT-IR spectrum of the BAPDPM is given in Fig. 1. The broad band at 3364 cm^{-1} indicates the symmetric stretching vibrations of the hydroxyl group. The small band at 3286 cm^{-1} is due to the symmetric –NH stretching vibrations of the secondary amide group and the strong band at 1669 cm^{-1} corresponds to the symmetric stretching vibrations of C=O group of the amide group. The band at 2793 cm^{-1} indicates the presence of bridging –CH group. ^{1}H-NMR spectrum is shown in Fig. 2. The peak at 5.2 ppm corresponds to the highly shielded bridging –CH group which confirms the formation of this compound. The singlet at 8.8 ppm is due to the presence of the much shielded –NH protons and the broad peak at 10 ppm indicates the presence of
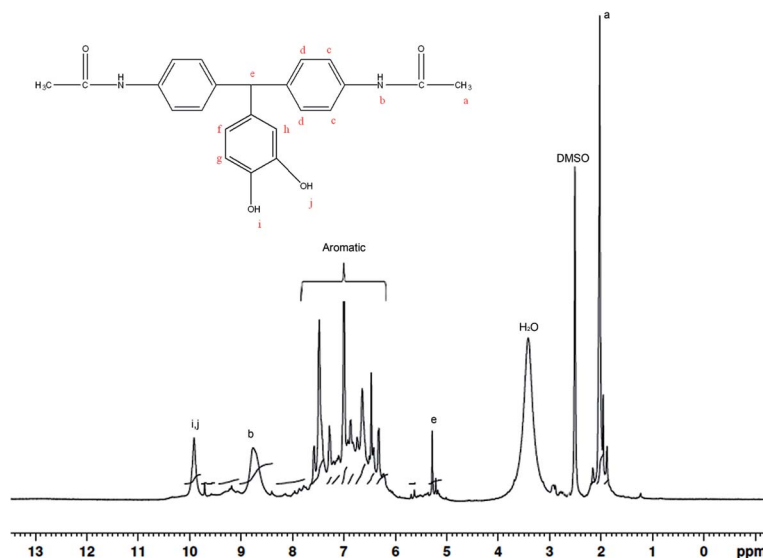

Fig. 2 ^{1}H-NMR spectrum of BAPDPM.

both –OH protons. All the aromatic proton peaks appear between 7.2 and 9 ppm.

In the second step, the long mono bromo aryl pendent group BPQMK was prepared by the nucleophilic substitution reaction of 8-hydroxy quinoline with 2,4′-dibromo acetophenone in the presence of anhydrous potassium carbonate as base and a catalytic amount of potassium iodide in DMF. The FT-IR spectrum of BPQMK is given in Fig. 1. The strong band at 1246 cm^{-1} is assigned to the stretching vibration of aryl alkyl C–O–C group indicating the formation of bond. The band at 1666 cm^{-1} is due to the symmetric stretching vibrations of the C=O group. The aromatic and aliphatic C–H stretching vibrations appear as strong bands at 3061 cm^{-1} and 2923 cm^{-1} respectively.

In the third step, the BAAPQMCPM which contains amide linkages and pendent groups was obtained using the classical Ullman etherification reaction, by the nucleophilic substitution reaction of BAPDPM with BPQMK in 1 : 2 mole ratio in the presence of anhydrous potassium carbonate and a pinch of copper powder at 160 °C in NMP as solvent. The copper powder here is used to facilitate the formation of phenoxy ion nucleophile and to assist the removal of bromine from the aromatic ring as there is no strong activation in the ortho and para positions except that of ketone group. The FT-IR spectrum of the compound is shown in Fig. 1. The secondary amide N–H group stretching vibrations appear at 3302 cm^{-1} and the band at 2862 cm^{-1} is assigned to the bridging methine and methylene groups. The strong band at 1659 cm^{-1} is due to the symmetric stretching vibrations of the amide C=O group and the ketonic C=O group. The two strong bands at 1072,

1250 cm^{-1} are attributed to the stretching vibration of aryl alkyl C–O–C group. In the ^{1}H-NMR spectrum the peak at 9.92 ppm is assigned to the highly shielded –NH proton. The methine and methylene peaks appear at 5.4 and 6.9 ppm respectively. Aromatic protons are shielded and shifted to down field between 7 ppm and 9 ppm. Highly shielded protons attached to the carbon neighbouring to the nitrogen in the quinoline ring is downshifted to 8.93 ppm.

The diamine monomer BAPQMCPM was prepared by the basic hydrolysis of the diamide compound in ethanol as solvent under reflux condition followed by the careful neutralization and precipitation to prevent soluble amine salt formation. The detailed reaction scheme for the synthesis of the diamine is shown in Scheme 1. In ^{1}H-NMR spectrum of the BAPQMCPM (Fig. 3) the peaks between 6.3 ppm and 9 ppm are assigned to the aromatic protons. Here an up-field shift is observed when the amide group is hydrolysed to amine group. The peak at 2.9 ppm corresponds to –NH$_2$ group. The peak at 5.3 ppm represents the highly shielded –CH group. The peak at 6.7 ppm corresponds to –CH$_2$ linkages in the pendent groups. The electron withdrawing oxygen and carbonyl linkages attached to the methylene group shift the peak to low field and so that the peaks appear at higher value. A higher resonance value (8.85 ppm) is observed for the aromatic C–H neighbouring to the nitrogen in the quinoline moiety. The ^{13}C-NMR spectrum of the diamine BAPQMCPM (Fig. 4) is consistent with the proposed structure. The aromatic carbons appear in the range 110–170 ppm. The resonances at 72.95, and 89.3 ppm may be assigned to the methylene and the methine group respectively.
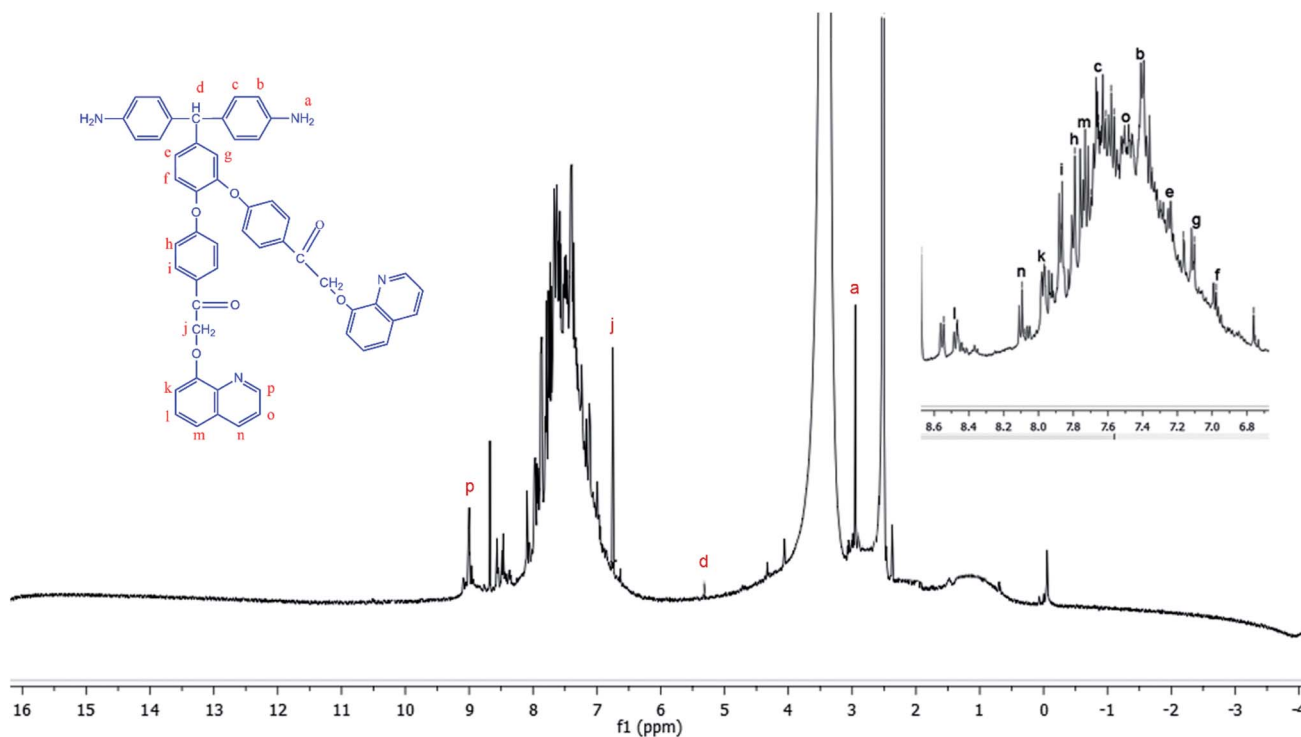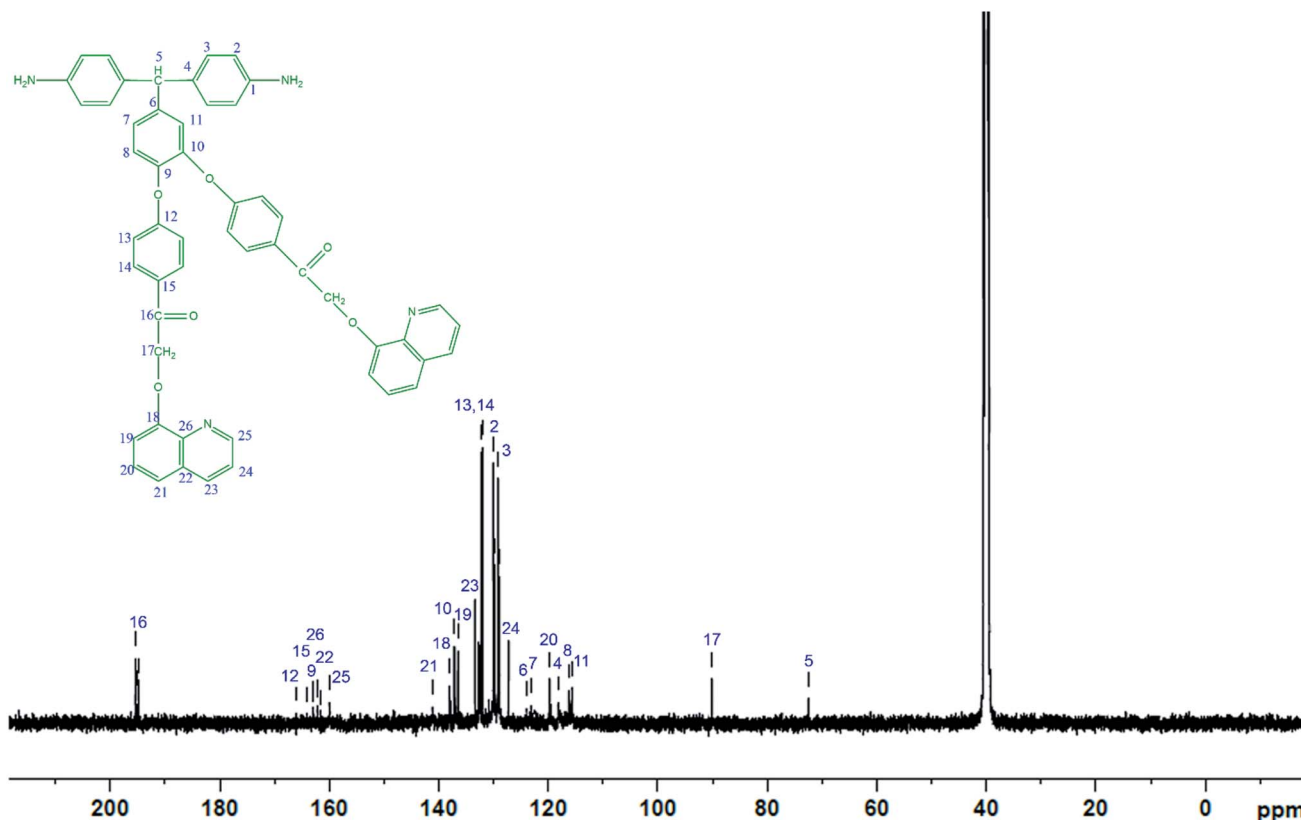

Fig. 3 ^{1}H-NMR spectrum of BAPDPM.

Fig. 4 ^{13}C-NMR spectrum of the diamine BAPQMCPM.

The carbonyl groups in the pendent group are represented by the peak around 194 ppm.

Preparation and characterization of aromatic amino functionalized silica

Aromatic amino functionalized nano silica was prepared by a procedure reported by Ghorpade *et al.*[40] in 2015 (ESI†). The nano silica particles were phenylated by the addition of phenyl triethoxy silane (PTEOS) to a mixture of triethylamine and nano silica suspension in toluene and subsequent reaction under reflux condition. The phenylated silica was nitrated using nitrating mixture (acetic acid + sodium nitrate) and separated by centrifugation and purified by repeated washings. The nitro phenyl functionalized silica was reduced to amino phenyl functionalized silica using stannous chloride in ethanol under reflux condition (Scheme S1, ESI†). The FT-IR analysis of nano particles confirm modification of nano silica with aromatic amino group. Fig. S1 (ESI†) shows the FT-IR spectra of aromatic nitro functionalized silica and aromatic amino functionalized silica. The characteristic bands at 1065 cm^{-1} and 961 cm^{-1} show the stretching vibrations of Si–O–Si group.[42] The band at 1651 cm^{-1} is due to the bending vibrations of the residual water molecules adsorbed on the surface of SiO$_2$. The bands at 1596 cm^{-1} and 1342 cm^{-1} indicate the presence of nitro groups. The wide band around 3400 cm^{-1} is due to the asymmetric stretching vibrations of the amino and Si–OH groups which confirm the reduction of nitro group to amino group.[43]

XPS analysis was performed to confirm the chemical states of elements in the aromatic amino and nitro functionalized silica. The XPS results of the aromatic amino functionalized silica are presented in Fig. S2 (ESI†). In the XPS spectra of both amino and nitro functionalized silica, O 1s, Si 2p, C 1s and N 1s peaks are found. In the XPS spectra of aromatic amino functionalized silica, the N 1s peak is at 397 eV, the C 1s is present around 287 eV, the Si 2p peak is around 104 eV, Si 2s peak is around 154 eV and the O 1s peak is around 533 eV. The small peak of N 1s which appeared at 407 eV in the aromatic nitro functionalized silica, shifts to 397 eV confirming the change in the chemical states of nitrogen due to the conversion of nitro group to amino group. The C 1s peak around 287 eV represents the phenyl group in the aromatic amino functionalized silica.[40]

Preparation and characterization of polyimides and their nanocomposites with aromatic amino functionalized silica

The polyimide containing long pendent chains was prepared by the conventional two step method. In the first step, which is an exothermic reaction, an equimolar amount of BAPQMCPM and BTDA (or BPADA) in a solution of 20 w% solid concentration containing in NMP were reacted. The resultant viscous solution of polyamic acid was converted into the corresponding polyimide by thermal and chemical imidization methods. In the thermal imidization method, the solvent evaporation was carried out at 80 °C for overnight and sequential heating at temperatures of 120 °C, 150 °C, 200 °C, 250 °C, 300 °C for half
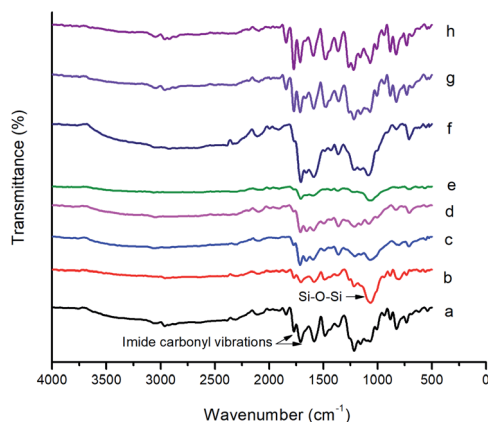
Fig. 5 FT-IR spectra of PIs and nanocomposites (a) BAPQMCPM-BPADA PI (b) BAPQMCPM-BPADA PI/2%F-silica, (c) BAPQMCPM-BPADA PI/5%F-silica, (d) BAPQMCPM-BPADA PI/10%F-silica, (e) BAPQMCPM-BTDA PI, (f) BAPQMCPM-BTDA PI/2%F-silica, (g) BAPQMCPM-BTDA PI/5%F-silica, (h) BAPQMCPM-BTDA PI/10%F-silica.

an hour at each temperature was carried out to convert to the fully imidized structure. Clear, continuous, creasable film was obtained. In the chemical imidization method, acetic anhydride and pyridine were added to the poly(amic acid) solution in 2 : 1 volume ratio and the mixture was stirred at 100 °C for 8 hours to achieve complete imidization.

BAPQMCPM-PI-functionalized silica nanocomposites were synthesized by the two-step thermal imidization method. The reaction mixture of diamine and BTDA (or BPADA) was stirred in NMP at room temperature in nitrogen atmosphere for 24 hours to get a viscous polyamic acid solution. A suspension of various ratios of aromatic amino functionalized silica (2, 5, 10% by weight) taken separately in NMP were mixed with poly(amic acid) solution, sonicated and kept at 120 °C, 150 °C, 200 °C, 250 °C for one hour at each temperature and at 275 °C and 300 °C for half an hour each to complete the thermal imidization. Clear, creasable composite films were formed.

The FT-IR spectra of BAPQMCPM/BTDA-PI, BAPQMCPM/BPADA-PI and their nanocomposites are shown in Fig. 5. The bands at 1773–1779 cm^{-1} and 1705–1713 cm^{-1} indicate the presence of imide carbonyl groups. The C–N stretching of imide group was observed at 1363 cm^{-1} C–N bending vibrations give band at 754 cm^{-1}. The band around 1665 cm^{-1} represents the BTDA carbonyl group and that around 1589 cm^{-1} is due to the presence of carbonyl in the diamine. In the polyimide nanocomposites the characteristic band due to Si–O–Si linkage appears at 1040–1080 cm^{-1}. The band around 3040–3060 cm^{-1}

is due to the stretching vibrations of the Ar–H bond. Around 2920–2970 cm^{-1} all kinds of C–H vibrations (methine, methylene, isopropylidene) are found.[37,42,44,45]

The chemical structure of the polyimides was also confirmed by ^{1}H-NMR spectroscopy (Fig. S3a and b, ESI†). The complete imidization of the poly(amic acid) was also confirmed by the absence of residual resonance in the region 3–4.2 ppm indicating the absence of amine protons. The BPADA based polyimide shows the characteristic peak of isopropylidene group at 2.8 ppm. In BTDA based PI the peaks at 6.2 and 5.5 ppm indicate the methylene and methine groups respectively. But the peaks of methylene and methine groups are present around 6.9 and 5.3 ppm respectively in BPADA based polyimide.

Properties of polyimides and nanocomposites

Intrinsic viscosity and molecular weight. The intrinsic viscosity of the polyimides was measured at room temperature using DMAc as solvent using an Ubbelohde viscometer at a concentration of 0.5 g dL^{-1}. The intrinsic viscosity of BTDA based polyimide is 1.5 dL g^{-1} and that of BPADA based polyimide is 2.1 dL g^{-1}. Both values show fairly high molecular weight. The same kind of polyimides with high intrinsic viscosity was reported by Wang et al.[46] Similarly, star branched polyimides with high inherent viscosity were reported by Wu et al. in 2017 and Liu et al. in 2016.[47,48] The molecular weights of these PIs determined by GPC in DMF relative to polystyrene standards were in the range of 91 868–98 246 for M_w and 42 868–44 542 for M_n with M_w/M_n values of 2.1–2.2.[11,49] Polyimides show good film forming capacity and are creasable due to the formation of high molecular weight polymer.

UV-visible spectroscopy-optical properties. The absorption spectra recorded in dilute DMAc solution (1.25 mol L^{-1}) were analysed (Fig. S4, ESI†) and cut off wavelength (absorption edge λ_0) values are given in Table 1. The cut off wavelength observed in UV-visible spectra is the measure of colour intensity of polyimides and it depends on the electronic structure of the diamine and dianhydride used in the polyimide synthesis. Both of the polyimides show absorption of light at wavelengths shorter than the 350 nm, in the UV region, indicating good transparency. Most of the conventional polyimides show dark colouration due to the conjugated aromatic structure and the formation of charge transfer complex. But here, the long and bulky aryl pendent groups and flexible linkages reduce intermolecular interaction between different chains and prevent the charge transfer complex formation and consequently polyimides are transparent. Even then these polyimides are not colourless, because of the presence of a number of aromatic

Table 1 Mechanical properties, UV-visible spectral data, molecular weight & intrinsic viscosity of PI

PI & codes	Tensile strength (MPa)	Tensile elongation at break point (%)	UV λ_{max} (nm)	Intrinsic viscosity (dL g^{-1})	Number average molecular weight (M_n)	Weight average molecular weight (M_w)	M_w/M_n
BAPQMCPM-BTDA	17	133.5	325	1.5	42 868	91 538	2.14
BAPQMCPM-BPADA	13	155.3	330	2.1	44 542	98 246	2.21

groups in the main chain as well as in the pendent chains. BPADA based polyimide absorbs at lower wavelengths of absorption owing to the greater number of ether linkages which increases the segmental motion in the main chain.[50,51]

Mechanical properties. The mechanical properties of all polyimide films were analysed with a universal testing machine of Instron model 1130 tensile tester using a 5 kg load cell at a cross head speed of 5 mm min^{-1}. A dog-bone shaped films of 1 mm thickness, 40 mm length and a width of 20 mm (15 mm × 5 mm at the gauge section) were used for the analysis. All thermoplastic polyimides show a linear elastic deformation at small strains in the elastic region and a nonlinear or plastic deformation at large strain. The tensile stress and the elongation at break point of pure polyimides based on both BTDA and BPADA are given in Table 1. The elongation at break of pure polyimides based on both BTDA and BPADA are 133% and 155% respectively, indicating good flexibility, stretchability and ductility. The BPADA based polyimides show higher elongation at break due to the increased chain length and the presence of extra number of ether linkages in the main chain along with flexible isopropyl linkages causing better segmental rotation. Here, the elongation is less compared to that in our previously published work in which one long aromatic pendent group is present.[27] In 2007 Wang *et al.*[8] reported that poly etherimides with multiple alkyl side chains (number of CH$_2$ groups in each chain varies from 5 to 18) showed very high elongation at break (200–470%). Tensile strength of those polyimides was found to be low. In our work also the tensile strength is very low, when compared to the conventional polyimides. This may be due to the fact that most of the elastomers are with low tensile strength which is around 3 MPa.[24] Literature showed that un-vulcanized natural rubber without any filler content showed a tensile strength of 0.56 MPa.[52,53] In our work, these polyimides with multiple aromatic side chains also show low tensile strength. Here, the rigidity may be slightly high, as there are a greater number of aromatic groups in two side chains together. The presence of two bulky and long pendent groups inhibit the intermolecular attraction and cohesive forces to make the formation of charge transfer complex impossible and generate greater amount of free volume. Also, the *meta* substitution of one of the pendent groups on the central benzene ring introduces more asymmetry. The aromatic pendent moieties will push the neighbouring molecular chains apart to disrupt the crystalline packing.[54] The crystalline lattice formation between the pendent groups are also prohibited owing to the presence of flexible linkages in the side chains as they improve the segmental rotations in the same. These factors are attributed to the formation of highly amorphous polyimide matrix which improves overall flexibility and sustain good toughness.

Solubility. The solubility test was done by mixing 10 mg of polyimide in 1 mL of solvent at room temperature and allowing to stand for 24 hours. If the polyimide was insoluble under cold conditions, then it was heated and cooled. The chemically imidized polyimides exhibited partial solubility in common organic solvents such as ethanol, methanol and THF at room temperature and at hot conditions. But they show improved solubility in chloroform, dichloromethane and acetone when they are kept for 24 hours and in hot condition. They are completely soluble in polar aprotic, solvents like DMF, DMAc, DMSO, and NMP even at room temperature. BPADA based polyimides are showing good solubility in THF at room temperature. BTDA polyimides show less solubility due to the absence of ether linkages in the chain backbone when compared to the BPADA based polyimides. Enhanced solubility of polyimides is attributed to the combined effect of the presence of flexible linkages along with bulky/long aryl pendent groups and meta substitution.[48,55,56] All these factors reduce the intermolecular, interchain interaction and cohesive forces, thereby prevent close packing and crystallinity which increase the available free volume so that solvent molecules can diffuse in that space interacting with different polar groups, enhancing solubility. Good solubility in low boiling point solvents is desirable in the manufacture of low-temperature processable materials for advanced micro electronics.[57] Thermally imidized polyimide is insoluble in solvents and the reason may be the crosslinks formed between different chains by the disruption of some of the double bonds of the carbonyl groups at the higher temperatures. Conventional polyimides show very poor solubility in low boiling organic solvents. But Wang *et al.* in 2007[8] showed that the polyetherimides with multiple alkyl side chains exhibit very good solubility in low boiling chlorinated solvents and in all high boiling solvents. Recent studies show that polyimides with aromatic pendent groups along with flexible linkages have improved solubility.[55]

Morphology. The surface morphology of prepared polyimides and nanocomposites were studied using scanning electron microscopy of the fractured surface of the material and is displayed in Fig. 6 and S5(a–e) (ESI†). The polyimide hybrid nanocomposite with nano silica particles shows a rough and uneven surface. The SEM images show the uniform and effective dispersion of aromatic amino functionalized silica nano particles in the polyimide matrix. The aromatic amino functionalized silica nanoparticles are mostly spherical and triangular in nature and the size distribution is uneven. The nano particle size distribution is between 75–120 nm. Usually, the inorganic nano particle phase does not easily disperse in polymer matrix due to their high surface energy. Here, the micrographs show that there is a homogeneous distribution of nano silica particles in the polyimide matrix without any
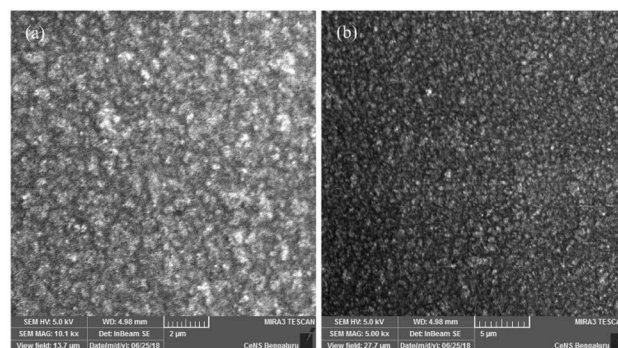

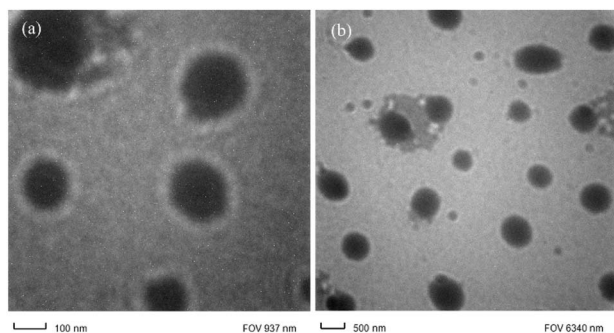Fig. 6 SEM micrographs of BAPQMCPM–BTDA PI/2%F-silica.

Fig. 7   TEM micrographs of BAPQMCPM-BTDA PI/2%F-silica.

agglomeration when the weight percentage of silica is 2%. The reason is that the amino groups present on the surface of the silica nano particles form covalent bonds with the polyimide matrix and inhibit agglomeration. So, there will be better interfacial interaction and compatibility between the functionalized silica nano particles and the polyimide matrix, compared to the nano composites formed between unmodified silica nanoparticles and polyimide matrix. But with 10 wt% aromatic amino functionalized silica the nanoparticles are dispersed well in the polyimide matrix with slight agglomeration as shown in Fig. S5(d and e).† As the weight percentage of nanoparticles increases it ends with agglomeration normally.[58] But here also, the covalent bonding between the aromatic amino functionalized silica and the main chain of polyimide reduces the agglomeration.[37,43]

Transmission electron microscopy (TEM) analysis was performed for nanocomposite with 2% functionalized silica, to analyze the microstructure and internal composition related to the size, shape and pattern of distribution in the polyimide matrix. Here, the light portion of the image shows the polyimide matrix part and the dark spots are the modified silica particles (Fig. 7 and S6a–i, ESI†). The modification of the silica particles plays an important role in the uniform distribution of the particles in the matrix. Here, it is observed that the aromatic amino modified silica nano particles are dispersed homogeneously in the polyimide matrix without showing any signs of aggregation. This is due to the covalent bonding between amino group of silica particle and carboxyl group of polyamic acid during the mixing and curing stage. Thus, the compatibility between polymer chain and nanoparticles is enhanced. Here the dark spherical silica particles are uniformly distributed or dispersed in nanometre range (about 50–200 nm size). There is no aggregation of the silica particles, showing uniform distribution.[35]

Crystallinity. The prepared polyimides and nano composites were characterized by X-Ray diffraction analysis using monochromatic radiation with 2 theta ranging from 5° to 70°. Fig. 8 shows the XRD patterns of the polyimide/SiO$_2$ nanocomposites with varying contents of silica. The broad halo in the XRD patterns of pure polyimides shows that polyimides are in the amorphous state only. The amorphous nature of the polyimides could be attributed to the presence of pendent aryl chains and ether and ketone linkages in the backbone. The flexible linkages improve the segmental rotation while the bulky aryl pendent
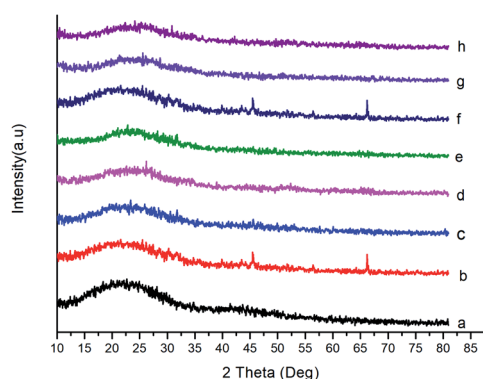

Fig. 8   XRD patterns of PIs and nanocomposites (A) BAPQMCPM-BPADA PI (B) BAPQMCPM-BPADA PI/2%F-silica, (C) BAPQMCPM-BPADA PI/5%F-silica, (D) BAPQMCPM-BPADA PI/10%F-silica, (E) BAPQMCPM-BTDA PI, (F) BAPQMCPM-BTDA PI/2%F-silica, (G) BAPQMCPM-BTDA PI/5%F-silica, (H) BAPQMCPM-BTDA PI/10%F-silica.
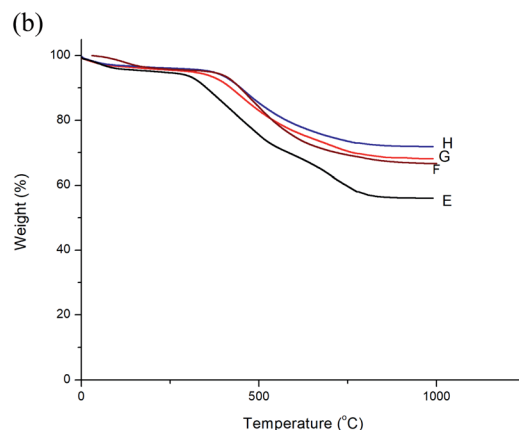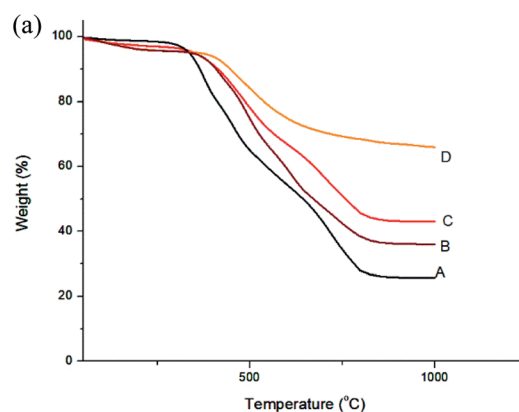
Fig. 9   (a) TGA curves of PIs and Nanocomposites (A) BAPQMCPM-BPADA PI (B) BAPQMCPM-BPADA PI/2%F-silica, (C) BAPQMCPM-BPADA PI/5%F-silica, (D) BAPQMCPM-BPADA PI/10%F-silica. (b) TGA curves of PIs and Nanocomposites (E) BAPQMCPM-BTDA PI, (F) BAPQMCPM-BTDA PI/2%F-silica, (G) BAPQMCPM-BTDA PI/5%F-silica (H) BAPQMCPM-BTDA PI/10% F-silica.

Table 2 Thermal & electrical data of PI/F silica nanocomposites

PI & nanocomposites codes	T_g (°C)	$T_{10\%}$ (°C)	CY (%)	LOI	Dielectric constant at 1 MHz
BAPQMCPM-BTDA	156	388	57.0	40.3	2.8
BAPQMCPM-BTDA2% nanosilica	220	447	66.0	44.0	4.0
BAPQMCPM-BTDA5% nanosilica	263	454	69.0	45.1	4.4
BAPQMCPM-BTDA10% nanosilica	280	481	72.0	46.3	5.7
BAPQMCPM-BPADA	130	364	27.0	28.3	2.5
BAPQMCPM-BPADA2% nanosilica	165	409	38.0	32.7	3.0
BAPQMCPM-BPADA5% nanosilica	180	413	45.0	35.5	4.2
BAPQMCPM-BPADA10% nanosilica	235	450	67.0	44.3	5.3

groups inhibit the inter chain interactions and restrict close packing of polymer chains resulting in a complete randomness and there by highly amorphous structure is observed. Here, the position of halo maximum can be considered as most probable intersegmental distance between polymer chains.[59] The d-spacing for BTDA based polymer is 3.86 Å and that of BPADA based polyimide is 4.2 Å. In BPADA based polyimide, more free volume is generated due to the extended chain length along with aliphatic isopropylidene group and ether linkages. Also, the presence of long side chains can lead to the formation of separate layered crystalline structure. But here, the formation of separate, regularly arranged layers of crystalline structures may be prevented due to the flexible linkages present between the aromatic groups in the side chains. All the nanocomposites are also in highly amorphous state and the broadness of halo of nanocomposites increases when compared to that of pure polyimide.[45]

Thermal properties. Thermal stability of polyimides and nanocomposites was investigated using TGA at a heating rate of 10 °C min⁻¹ in nitrogen atmosphere (Fig. 9). The $T_{10\%}$ and char yields at 1000 °C were calculated from thermo grams and the data are presented in Table 2. The $T_{10\%}$ values are in the range of 364–482 °C indicating very good thermal stability. Weight loss observed around 250–300 °C may be due to the decomposition of carbonyl and methylene groups. When temperature is

raised above 300 °C, an inflection is shown which may be due to the breakage of isopropyl group. Above 500 °C the imide ring may be undergoing decomposition. The flexible ether and ketone and isopropyl linkage in the chain backbone and the packing disruptive long/bulky side chain, which decrease total crystallinity are expected to reduce the thermal stability and flame resistance of the polyimide and nano composites. But, the aromatic groups and the ether linkages in the pendent group are able to retain high thermal stability.[6,10] It is confirmed that the presence of alkyl pendent groups in the polyimides cause the deterioration of thermal properties[8] but bulky aryl side chains with flexible linkages can retain those good heat resistant properties but presence of heteroaromatic ring in the side chain decrease the thermal stability slightly.[55] Nanocomposites exhibit enhanced thermal stability than pure polyimides. As the percentage of nano filler increases, decomposition temperature increases because of the high thermal stability imparted by the silica which also acts as the heat sink absorbing heat, reducing heat transfer to the material and there by inhibiting the decomposition, protecting the PI matrix.[60] Also, the functionalization of silica nano powder is carried out by the aromatic amino groups which improve and maintain the rigidity as well as the thermal stability of the polyimide matrix.[40]

The glass transition temperature of polyimides and nanocomposites were determined using DSC at a heating rate of 10 °C min⁻¹ in nitrogen atmosphere. The DSC curves of BTDA based polyimides are shown in Fig. 10 and those of BPADA based polyimides are given as Fig. S7 (ESI†). The values are listed in Table 2. The glass transition temperature depends upon the onset of segmental motion in a polymer molecule which in turn depends upon the molecular structure and geometry of the polymer molecule. The bulky aryl pendent groups decrease cohesive forces and inhibit the chain packing and generate greater free volume. The flexible ether and ketone linkages in the main chain improves the segmental motion so that it starts at an early stage thereby reducing T_g. The flexible linkages in the pendent groups improve the localised movements in the pendent chains. So the combined influence of both bulky aryl pendent groups and the flexible linkages in the chain backbone as well as in the pendent groups improves the available free volume so that the segmental motion starts at an early stage reducing the T_g to a greater extent.[50,60,61] It is reported that, highly branched aromatic polyimides show lower T_g than
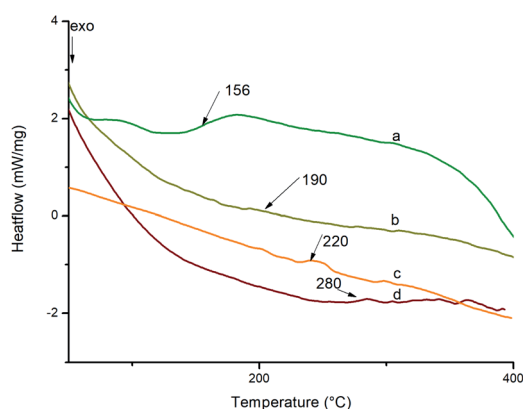

Fig. 10 (a)BAPQMCPM-BTDA PI, (b) BAPQMCPM-BTDA PI/2%F-silica, (c) BAPQMCPM-BTDA PI/5%F-silica, (d) BAPQMCPM-BTDA PI/10%F-silica.

the conventional PIs due to the improved free volume. The T_g values of BPADA based polyimides and nanocomposites are lesser than that of BTDA based polyimides and nano-composites. This is due to the presence of two ether linkages in the chain backbone along with the isopropyl group, which give more segmental rotations whereas there is only a carbonyl group present in the chain backbone of BTDA based polyimides and nanocomposites. Also, the extended chain length of the BPADA based polyimides improves the free volume. It is observed that, as the percentage of silicon dioxide nano filler increases, T_g values also increases. This is consequence of the higher rigidity imparted by aromatic amino functionalized silica which occupy the available space between the chains hindering the chain mobility and reducing the total free volume, thereby the segmental motion starts at a relatively higher temperature.

Flame retardancy. The amount of char yield under N_2 atmosphere at 1000 °C is evaluated from TGA diagrams for polyimides and nanocomposites. For BTDA based polyimide and nanocomposites it is 57–72% which indicate the very high flame resistance of the polymers. BPADA based polyimides and nanocomposites show lesser char yield values (27–66%). Generally, the char yield can be applied as a factor for estimating limiting oxygen index (LOI) of the polymers based on van Krevelen and Hoftyzer equation LOI = 17.5 + 0.4CR (where CR is the char yield). High char yield can be ascribed to the high aromatic content of the polyimides and nanocomposites.[62] The LOI values of polymer should be above the threshold value of 26 which render them self-extinguishing, a valuable property for many applications where high flame resistance are required.[63] The LOI values of polyimide and nanocomposites are between 27 and 47 indicating high flame resistance with good self-extinguishing property. Here, the silica nano particles enhance the flame retardancy of polyimides.[33]

Electrical properties. The dielectric properties of polyimide and nanocomposites were measured in the varying frequency range of 100 Hz to 1 MHz at room temperature and is given in Table 2. The dielectric constant is a function of polarity and number of polarizable groups in an applied electric field and fractional free volume or the (porosity) in the polymer matrix.[64] As the frequency changes from lower to higher values, the capacitance, dielectric constant and dissipation factor decreased remarkably. Each diamine and dianhydride units of polyimide chains contain a number of polar groups, aromatic rings and so the capacitance as well as dielectric constants might be moderate or high. At 1 MHz, the polyimides show very low dielectric constants while nanocomposites show increased dielectric constants as the percentage of aromatic amino functionalized silica nano filler increases. Aromatic rings, oxygen and nitrogen containing bonds increase the polarizability due to the loosely attached pi electrons and lone pair of electrons respectively. But the key factor here is the increased free volume between polyimide chains created by the presence of long and bulky pendent groups resulting in lower density of dipole moments (the number of polarizable groups per unit volume) and so the dielectric properties can be lowered very much. The BPADA based polyimides show slightly lower dielectric constant

as a consequence of the lower conjugation and extra free volume generated by the extended chain length of the same with ether and aromatic groups. Usually dielectric constant increases with the increasing silica content at a constant temperature.[65] When aromatic amino functionalized nano silica powder is added, it establishes good chemical bonds with polyimide matrix and thus total free volume between the chains decreases. Also, the number of polarizable groups per unit volume increases owing to the aromatic amino groups. So these two factors can enhance the electrical properties of nanocomposites.[66,67]

Conclusions

In summary, two novel flexible/stretchable polyimides were successfully synthesized by reacting a new diamine containing two long/bulky aromatic pendent chains and flexible linkages, with commercially available tetra carboxylic acid dianhydrides. Nanocomposites of polyimides were prepared with aromatic amine functionalized silica and characterized. SEM analysis shows a uniform distribution and better compatibility of the functionalized silica nanopowder in polyimide matrix. The neat polyimides show good elongation at break (133–155%) but low tensile strength. TGA shows that both the polyimides ($T_{10\%}$ = 364 & 388) and nanocomposites ($T_{10\%}$ = 409–482 °C) have high thermal stability. LOI values of both polyimides and nanocomposites are above 28, which indicate good self-extinguishing property. DSC analysis revealed very low T_g values for neat polyimides (130 °C and 156 °C) and for nanocomposites between 165–280 °C. Polyimides show very low dielectric constants (2.8 & 2.5) at 1 MHz showing good insulation property but the nanocomposites display higher dielectric constants (3–5.7 at 1 MHz). The prepared polyimides exhibit a better thermal stability, compared to the low thermal stability of polyimides with wholly alkyl side chains, which is attributed to the incorporation of aromatic groups in the bulky and long pendent chains. The lower T_g values for neat polyimides are ascribed to the improved segmental rotation by virtue of the flexible linkages in the enhanced free volume generated by the bulky pendent groups while nanocomposites show higher T_g due to the interrupted segmental rotation by the silica nano-filler. The enhancement in the thermal and electrical properties of the nanocomposites is ascribed to the covalent bond formation between the amino groups on the surface of silica nanoparticles with the polyimide molecules. It has been observed that incorporation of bulky aromatic side chains along with flexible linkages can improve the flexibility and elongation at break, enhance solubility, maintain optimum T_g, good thermal stability, high flame resistance and low dielectric constants. The combined effect of all these factors makes these polyimides an attractive candidate for microelectronics applications. Both the polyimides and nanocomposites can have various usages in process industries, aero-space and defence.

Conflicts of interest

There are no conflicts to declare.

Acknowledgements

References

1 D. J. Liaw, K. L. Wang, Y. C. Huang, K. R. Lee, J. Y. Lai and C. S. Ha, *Prog. Polym. Sci.*, 2012, **37**, 907–974.

2 M. Ghosh and K. Mittal, *Polyimides: Fundamental and Application*, Marcel Dekker, New York, 1996.

3 P. Ma, C. Dai, H. Wang, Z. Li, H. Liu, W. Li and C. Yang, *Compos. Commun.*, 2019, **16**, 84–93.

4 A. Ghosh, S. K. Sen, S. Banerjee and B. Voit, *RSC Adv.*, 2012, **2**, 5900–5926.

5 W. J. Bae, M. K. Kovalev, F. Kalinina, M. Kim and C. Cho, *Polymer*, 2016, **105**, 124–132.

6 N. Amutha, S. A. Tharakan and M. Sarojadevi, *Macromol. Symp.*, 2016, **362**, 26–38.

7 R. Hariharan, S. Bhuvana, N. Amutha and M. Sarojadevi, *High Perform. Polym.*, 2006, **18**, 893–905.

8 D. H. Wang, Z. Shen, S. Z. D. Cheng and F. W. Harris, *Polymer*, 2007, **48**, 2572–2584.

9 M. Ghaemy and R. Alizadeh, *Eur. Polym. J.*, 2009, **45**, 1681–1688.

10 C. Wang, S. Cao, W. Chen, C. Xu, X. Zhao, J. Li and Q. Ren, *RSC Adv.*, 2017, **7**, 26420–26427.

11 Y. Liu, L. Liu, B. Ren, X. Zhu, W. Zhou and W. Li, *Dyes Pigm.*, 2019, **162**, 232–242.

12 P. Ma, C. Dai and H. Liu, *Polymers*, 2019, **19**, 555–562.

13 Q. Zhang, C. Y. Tsai, L. J. Li and D. J. Liaw, *Nat. Commun.*, 2019, **10**, 2–9.

14 S. H. Hsiao, S. C. Peng, Y. R. Kung, C. M. Leu and T. M. Lee, *Eur. Polym. J.*, 2015, **73**, 50–64.

15 Y. Tian, Y. Song, H. Yao, H. Yu, H. Tan, N. Song, K. Shi, B. Zhang, S. Zhu and S. Guan, *Dyes Pigm.*, 2019, **163**, 190–196.

16 D. Ai, H. Li, Y. Zhou, L. Ren, Z. Han, B. Yao, W. Zhou, L. Zhao, J. Xu and Q. Wang, *Adv. Energy Mater.*, 2020, **1903881**, 1–7.

17 C. L. Tsai, H. J. Yen and G. S. Liou, *React. Funct. Polym.*, 2016, **108**, 2–30.

18 J. C. Chen, J. A. Wu, C. Y. Lee, M. C. Tsai and K. H. Chen, *J. Membr. Sci.*, 2015, **483**, 144–154.

19 M. Hasegawa, *Polymers*, 2017, **9**(10), 520.

20 S. Kumar Sen and S. Banerjee, *RSC Adv.*, 2012, **2**, 6274–6289.

21 L. A. Bermejo, C. Alvarez, E. M. Maya, C. García, J. G. de la Campa and A. E. Lozano, *eXPRESS Polym. Lett.*, 2018, **12**, 479–489.

22 R. A. Shanks and I. Kong, in *Advances in Elastomers I. Advanced Structural Materials*, ed. P. M. Visakh, S. Thomas, A. K. Chandra and A. P. Mathew, Springer, Berlin, Heidelberg, 2013, ch. 2, vol. 11, pp. 11–45.

23 R. A. Rhein, *Thermally Stable Elastomers' A Review*, Naval Weapons Center, China Lake, California, 1983.

24 M. Ragin Ramdas, K. P. Vijayalakshmi, L. M. Munirathnamma, H. B. Ravikumar and K. S. Santhosh Kumar, *Mater. Today Commun.*, 2018, **17**, 180–186.

25 H. Chen, B. Hao, P. Ge and S. Chen, *Polym. Chem.*, 2020, **11**, 4741–4748.

26 M. Parmeggiani, P. Zaccagnini, S. Stassi, M. Fontana, S. Bianco, C. Nicosia, C. F. Pirri and A. Lamberti, *ACS Appl. Mater. Interfaces*, 2019, **11**, 33221–33230.

27 S. A. Tharakan, S. Raju, R. Balasubramaniam and S. Muthusamy, *Polym. Compos.*, 2019, **40**, 832–843.

28 D. Meis, A. Tena, S. Neumann, P. Georgopanos, T. Emmler, S. Shishatskiy, S. Rangou, V. Filiz and V. Abetz, *Polym. Chem.*, 2018, **9**, 3987–3999.

29 B. Deng, S. Zhang, C. Liu, W. Li, X. Zhang, H. Wei and C. Gong, *RSC Adv.*, 2018, **8**, 194–205.

30 S. Kango, S. Kalia, A. Celli, J. Njuguna, Y. Habibi and R. Kumar, *Prog. Polym. Sci.*, 2013, **38**, 1232–1261.

31 S. K. Kumar, B. C. Benicewicz, R. A. Vaia and K. I. Winey, *Macromolecules*, 2017, **50**, 714–731.

32 I. A. Rahman and V. Padavettan, *J. Nanomater.*, 2012, DOI: 10.1155/2012/132424.

33 S. Mallakpour and M. Naghdi, *Prog. Mater. Sci.*, 2018, **97**, 409–447.

34 Z. Hong, D. Wei, F. Yong, C. Hao, Y. Yang, J. Yu and L. Jin, *Mater. Sci. Eng., B*, 2016, **203**, 13–18.

35 Y. J. Kim, J. H. Kim, S. W. Ha, D. Kwon and J. K. Lee, *RSC Adv.*, 2014, **4**, 43371–43377.

36 K. H. Moon, B. Chae, K. S. Kim, S. W. Lee and Y. M. Jung, *Polymers*, 2019, **11**, 489–499.

37 M. Liang, Y. Wang, S. Sun and W. Yang, *J. Appl. Polym. Sci.*, 2020, **137**, 1–12.

38 T. Kang, I. Jang and S. G. Oh, *Colloids Surf., A*, 2016, **501**, 24–31.

39 T. Kang, J. H. Lee and S. G. Oh, *J. Ind. Eng. Chem.*, 2017, **46**, 289–297.

40 R. V. Ghorpade, C. R. Rajan, N. N. Chavan and S. Ponrathnam, *eXPRESS Polym. Lett.*, 2015, **9**, 469–479.

41 Y. Lin, S. Hu and G. Wu, *J. Phys. Chem. C*, 2019, **123**, 6616–6626.

42 Y. Zhao, X. Qi, Y. Dong, J. Ma, Q. Zhang, L. Song, Y. Yang and Q. Yang, *Tribol. Int.*, 2016, **103**, 599–608.

43 C. F. Cheng, H. H. Cheng, P. W. Cheng and Y. J. Lee, *Macromolecules*, 2006, **39**, 7583–7590.

44 X. Huang, B. Chen, M. Mei, H. Li, C. Liu and C. Wei, *Polymers*, 2017, **9**, 484–496.

45 H. Gao, D. Yorifuji, Z. Jiang and S. Ando, *Polymer*, 2014, **55**, 2848–2855.

46 D. H. Wang, Z. Shen, M. Guo, S. Z. D. Cheng and F. W. Harris, *Macromolecules*, 2007, **40**, 889–900.

47 F. Wu, X. Zhou and X. Yu, *RSC Adv.*, 2017, **7**, 35786–35794.

48 S. Liu, S. Zhu, X. Wang, H. Tan and S. Guan, *High Perform. Polym.*, 2017, **29**, 46–57.

49 Y. Zhou, G. Chen, H. Zhao, L. Song and X. Fang, *RSC Adv.*, 2015, **5**, 53926–53934.

50 Y. Chen, R. Huang, Q. Zhang, W. Sun and X. Liu, *High Perform. Polym.*, 2017, **29**, 68–76.

51 J. Yao, C. Wang, C. Tian, X. Zhao, H. Zhou, D. Wang and C. Chen, *Des. Monomers Polym.*, 2017, **20**, 449–457.

52 C. H. Chan, J. Joy, H. J. Maria and S. Thomas, in *Natural Rubber Materials Volume 2: Composites and Nanocomposites*, ed. S. Thomas, C. H. Chan, L. Pothen, J. Joy and H. J. Maria, Royal Society of Chemistry, London, 7th edn, 2013, ch. 1, vol. 2, pp. 1–33.

53 D. Ponnamma, R. Ramachandran, S. Hussain, R. Rajaraman, G. Amarendra, K. T. Varughese and S. Thomas, *Composites, Part A*, 2015, **77**, 164–171.

54 Y. Li, Y. Chu, R. Fang, S. Ding, Y. Wang, Y. Shen and A. Zheng, *Polymer*, 2012, **53**, 229–240.

55 L. Yi, W. Huang and D. Yan, *SJ. Polym. Sci., Part A: Polym. Chem.*, 2017, **55**, 533–559.

56 L. Yi, C. Li, W. Huang and D. Yan, *J. Polym. Sci., Part A: Polym. Chem.*, 2016, **54**, 976–984.

57 S. M. Amininasab, S. Esmaili, M. Taghavi and Z. Shami, *J. Fluorine Chem.*, 2016, **192**, 48–57.

58 Y. Shen and A. C. Lua, *Chem. Eng. J.*, 2012, **188**, 199–209.

59 T. Koley, P. Bandyopadhyay, A. K. Mohanty and S. Banerjee, *Eur. Polym. J.*, 2013, **49**, 4212–4223.

60 A. S. More, S. K. Pasale and P. P. Wadgaonkar, *Eur. Polym. J.*, 2010, **46**, 557–567.

61 A. S. More, A. S. Patil and P. P. Wadgaonkar, *Polym. Degrad. Stab.*, 2010, **95**, 837–844.

62 Y. Liu, Y. Zhang, Q. Lan, Z. Qin, S. Liu, C. Zhao, Z. Chi and J. Xu, *J. Polym. Sci., Part A: Polym. Chem.*, 2013, **51**, 1302–1314.

63 M. Fathima Rigana, R. Balasubramanian, S. Balaji and M. Sarojadevi, *Polym. Compos.*, 2019, **40**, 600–614.

64 X. Peng, W. Xu, L. Chen, Y. Ding, T. Xiong, S. Chen and H. Hou, *React. Funct. Polym.*, 2016, **106**, 93–98.

65 K. Deshmukh, M. B. Ahamed, K. K. Sadasivuni, D. Ponnamma, M. A. A. AlMaadeed, R. R. Deshmukh, S. K. K. Pasha, A. R. Polu and K. Chidambaram, *J. Appl. Polym. Sci.*, 2017, **134**, 1–11.

66 S. Chisca, V. E. Musteata, I. Sava and M. Bruma, *Eur. Polym. J.*, 2011, **47**, 1186–1197.

67 A. Zulkifli, in *Dielectric Materials*, ed. M. A. Silaghi, Intech, Croatia, 3rd edn, 2012, ch. 1, pp. 3–26.